MULTI-SCALE LIVER MODEL FOR INVESTIGATING THE ELECTRICAL PROPERTIES OF LIVER TISSUE

Submitted by

Zhang Xingchen

Supervised by

Associate Professor Ong Sim Heng

Associate Professor Chui Chee Kong

Department of Electrical & Computer Engineering

National University of Singapore

In partial fulfillment of the requirements for the Degree of Bachelor of Engineering

National University of Singapore

ABSTRACT

Liver resection remains as the only definitive treatment to cure liver cancer, but significant blood loss during the surgery poses a challenge to the surgeons. This blood loss during liver resection may be minimized by ablating the liver parenchyma using radiofrequency (RF) energy. However, despite the popularity of RF-assisted liver resection, it is difficult to estimate the optimal amount of RF energy to apply to stop blood flow. More RF energy than necessary may often be used to stop bleeding and this will result in increased liver damage. By understanding the electrical properties of liver under RF energy will provide insights on the optimal amount of RF energy to apply.

A multi-scale liver model is proposed to simulate the electrical behavior (bio-impedance) of liver tissue under RF energy. The multi-scale liver model consists of cell level, liver level and liver level. A probe circuit model is also included to mimic the electrode-electrolyte (electrode probe - liver tissue) interface. A simulation software is also developed using MATLAB GUI to visualize the bio-impedance of liver tissue under different frequencies and to better organize the simulation results. The simulated impedance against frequency graph follows the correlation with the experiment data obtained by Gabriel in 1996. The relationship between tissue temperature and bio-impedance is also examined so as to draw further insights on cell death in relation to bio-impedance as cell death occurs at 60 ℃.

ACKNOWLEDGMENT

I would like to express my greatest gratitude to my supervisors, Associate Professor ONG Sim Heng from Department of Electrical Engineering, Associate Professor CHUI Chee Kong from the Department of Mechanical Engineering and Associate Professor CHANG KY Stephen from the Department of Surgery for giving me the opportunity to embark on this interesting final year project. With their constant support and guidance, I was able to accomplish this multi-disciplinary work.

I would also like to thank Dr. HUANG Wei Hsuan for helping me to clarify some of my doubts and his PhD research provides huge amount of insights for my work.

CONTENTS

LIST OF FIGURES

Fig. 20 Simulation Software – Cell Tab

Fig. 21 Simulation Software – Lobule Tab

LIST OF TABLES

LIST OF SYMBOLS AND ABBREVIATIONS

RF – Radiofrequency

CUSA – Cavitron Ultrasonic Surgical Aspirator

Rn – Resistance of cell nucleus matrix

Cn – Capacitance value of cell nucleus membrane

Zlc – Complex resistance value of liver cell

Ricm – Resistance of intracellular matrix

N – Relative volume of liver cell

Rplasma – Resistance of blood plasma

Rrbc – Resistance of red blood cell

Crbc – Capacitance of red blood cell membrane

L – Relative volume of red blood cell in micro vessel

Rlecm – Resistance of lobule extracellular matrix

Clc – Capacitance of liver cell membrane

Zmv – Complex resistivity of micro vessel

K – Relative volume of red blood cell in blood vessel

Rtecm – Resistance of tissue extracellular matrix

Zlobule – Complex resistance of liver lobule

Clobule – Capacitance of liver lobule membrane

M – Relative volume of lobules in the tissue

Zvessel – Complex resistance blood vessel

Zprobe – Complex resistance of probe model

Rct – Charge transfer resistance

Rs – Solution resistance

Zcpa – Phase angle impedance

Pt – Platinum

TiN – Titanium Nitride

EIT – Electrical Impedance Tomography

CHAPTER 1. INTRODUCTION

1.1 Radiofrequency Energy

Radiofrequency (RF) has been widely used to treat liver cancers in the form of ablation and coagulation for resection. Intra-operative blood loss during liver resections can be minimized by ablating the liver parenchyma using energy. RF can coagulate liver tissue faster and RF-assisted liver resection is relatively easier to operate compared to other techniques. However, it is difficult to estimate the depth of the avascular plane and the time and amount of RF needed to produce reliable coagulation are unknown. Therefore, more RF energy than necessary may be inadvertently applied to arrest bleeding and this will result in increased liver damage.

1.2 Mode of Operation of RF-Assisted Resection

For radiofrequency-assisted liver resection, the electrodes are connected to a RF generator which supplies RF current. When the electrode touches the skin and RF current is supplied, there will be high frequency alternating currents in the range of 100 kHz to 3 MHz, which are capable of generating iconic agitation and increasing the cellular and tissue temperature. Radiofrequency-assisted liver resection induces necrosis in healthy liver tissue at the resection plane to seal vascular and biliary structures and thereby facilitate bloodless dissection of the

parenchyma during resection. This can produce a coagulated surface on the liver parenchyma along the resection margin, and then liver transaction can be performed using a scalpel. There are two modes of operations: mono-polar and bipolar.

In mono-polar technique, the two electrodes are the active electrode and return electrode. The active electrode is used to for cutting or coagulation while the return electrode is placed over a large area of the body. The current passes from the active electrode into the target tissue and then passes through the human body in a direct path with least resistance to the return electrode. Finally, the current is fed back to the generator through the return electrode. Since the active electrode has a much smaller cross-sectional area than the passive electrode, it has a much greater current density and this is used to heat the tissue.

For bipolar technique, both electrodes are arranged on the tip of a forceps. The two electrodes contact tissue in close proximity. The applied current passes from active electrode to the target tissue and immediately flows to the return electrode before back to the generator. With bipolar electrode, the current density on both electrodes is equally high. Therefore, both electrodes have the same heating effect. The bipolar mode requires considerably less power to achieve the same effect than the mono-polar mode.

1.3 Organization of Thesis

The first part introduces the radiofrequency energy and RF-assisted liver resection. The second chapter is background and motivation. This part talks about problems associated with RF-assisted liver resection----bleeding and different techniques to stop bleeding. Chapter 3 defines the scope of the report and how the project contributes to address the bleeding issue associated with RF-assisted liver resection. In the literature review, basic cell model is examined and it forms the building block of our multi-scale model. The effect of temperature and alternating current on liver cells are also reviewed. The liver anatomy is studied so as to better understand the suitability of multi-scale model to simulate liver structure. The commercially available RF-assisted resection devices are reviewed to understand the status of technology development and its limitations. A probe model is also researched to simulate the electrode-electrolyte interface. This probe model makes the multi-scale model complete. Finally in the literature review, the relationship between bio-impedance and temperature is examined so that insights on cell death can be provided through impedance modeling. Chapter 5 talks about the proposed multi-scale liver model in details which consists of liver cell, liver lobule, liver tissue and electrode. Chapter 6 introduces the simulation software programmed using MATLAB GUI which provides a more visual and easy-to-manage system for the multi-scale model. The simulation results are also discussed. The last section of the thesis is the future works and conclusion.

CHAPTER 2. BACKGROUND & MOTIVATION

2.1 Liver Cancer and Blood Loss

Around the world, liver cancer is the fourth commonest cancer and is the third leading cause of cancer deaths. In Singapore it is the fourth commonest cancer among men, and the third commonest gastrointestinal tract cancer among all. (SingHealth 2014) The treatment of liver cancer depends on the location of the tumor, number of tumors and the size of the tumor. Liver resection remains the gold standard for the treatment of both primary and secondary liver tumors. However, fewer patients are suitable for liver resections. Other treatment options include chemotherapy, radiotherapy, cryoablation, microwave coagulation therapy, laser-induced thermotherapy and radiofrequency ablation. Radiofrequency ablation is an image-guided technique that uses radiofrequency energy to heat and destroy cancer cells. It is only effective if the size of the tumor is small. Liver resection is the surgical removal of a portion of the liver and is performed if the tumors are confined in one region of the liver. However, the liver surgical procedure in the form of liver resection is very demanding as liver contains numerous tissues and a lot of blood passes through it. Blood loss is the major concern during surgery and huge amount of operation time is spent on stopping the bleeding. Efforts to minimize or eliminate operative bleeding have always been the primary focus throughout the history of liver surgery.

2.2 Different Techniques to Stop Bleeding

Haemostatic control is the major challenge facing liver resection and blood loss is associated with increased risk for postoperative complications. Many interventions have been applied to reduce or stop intra-operative bleeding during liver resection. These include vascular clamping, Harmonic Scalpel, Ultrasonic surgical aspirators, compressive bipolar diathermy, radiofrequency-assisted liver resection and so on.

2.2.1 Vascular Clamping

Vascular clamping is an efficient tool to minimize bleeding during parenchymal transaction but it has limitations due to hemodynamic consequences. There are different types of vascular clamping methods such as inflow or outflow occlusion and total, partial or selective clamping. Clamping may also be either continuous or intermittent.

Pringle Maneuver is the simplest and the most widely used method of liver vascular clamping. A large atraumatic flexible hemostat is used to clamp the hepatoduodenal ligament interrupting the flow of blood through the hepatic artery and the portal vein and thus helping to control bleeding from the liver. A left hepatic artery from the left gastric artery can also be clamped in order to totally occlude the arterial inflow. Individual vascular structures of the hepatoduodenal ligament can be identified separately and clamped. (Chouillard,

Gumbs et al. 2010)

Selective Clamping consists of selective clamping of a hepatic lobe, a section, or even a liver segment. It can limit the ischemic injury to the projected resection and to accurately demarcate anatomic territories by creating ischemic margins at the liver surface. Selective sectoral clamping is mainly used for right liver sections.

Total vascular exclusion is the most complete liver clamping method which exclude the liver from the splanchnic and systemic circulations. Identification and clamping of the accessory arteries is also necessary because an incomplete afferent clamping associated with an efferent clamping leads to liver congestion and hemorrhage.

2.2.2 Cavitron Ultrasonic Surgical Aspirator (CUSA)

It makes used of a process called cavitation that can destruct the cells with a high water content while preserving structures rich in collagen (low in water), such as blood vessels and nerves. The low frequency waves cause an implosion of the cell, due to a vaporization of intracellular water by forming vacuoles which then resonate with the vibrating tip of the instrument. With this technology, the liver parenchyma tissue is fragmented with ultrasonic energy and aspirated, thus exposing vascular structures that can be ligated or clipped with titanium hemoclips. (Poon 2007)

2.2.3 Stapler Hepatectomy

Staplers can be used in liver surgery for control of inflow and outflow vessels or to divide liver parenchyma. This is because staplers have the ability to close and transect part of an organ and at the same time, create anastomosis between tissues. It can replace the conventional technique of applying vascular clamp followed by suturing. The efficacy of staplers is mainly related to the characteristics of the cartridges. When sealing large vessels, a cartridge which is able to release more lines of smaller staples is required.

2.2.4 Harmonic Scalpel

When ultrasonic system is used at a higher vibrating range, it can result in cutting and coagulating effect at the tissue-instrument interface and they are called harmonic scalpels. It uses ultrasonically activated shears to seal small vessels between the vibrating blades. The cutting effect is due to the change in the state of water molecules of tissues from liquid to gas. The rapid change in the state of water results in a rapid change in the volume of cells leading to destruction of the cell wall. The cutting is also caused by the mechanical friction between the blade and the tissue. The coagulation effect is caused by the breaking the hydrogen bonds in protein and the generation of heat in the vibrating tissue which lead the protein denaturation. (Poon 2007)

2.2.5 Ligasure

This is another device designed to seal small vessels by a combination of compression pressure and bipolar radiofrequency energy. It can denature the collagen and elastin within the vessel wall and surrounding connective tissue. The sealing mechanism uses the body's collagen to change the nature of the vessel walls to eliminate its lumen. (Boni, Dionigi et al. 2009)

CHAPTER 3. SCOPE & OBJECTIVE

The scope of the study focuses on the mechanism of RF-Assisted liver resection and aims to provide insight on haemostatic control during the operation. The objective of the paper is to investigate the electrical properties (bio-impedance response) and temperature of the liver tissue under RF energy. A multi-scale circuit model is examined to study the bio-impedance and temperature of liver tissue, liver lobules and liver cells. An electrode-electrolyte (probe) interface is included to derive the transfer function and study the frequency response of the model. A software interface is also developed using MATLAB GUI for easy organization of simulation results and data.

By knowing the electrical properties and temperature response of the liver tissue under RF energy can help us determine the duration and amount of RF energy to apply so that we can optimize the coagulation of the liver resection margins and reduce the invasiveness and damage of RF-assisted liver resection procedure.

CHAPTER 4. LITERATURE REVIEW

4.1 Basic Cell Model

The electrical model proposed by Fricke (Fricke, 1925) provides a good estimation of the electrical properties of a single cell as shown in the figure 4. In this model, every infinitesimal portion of the extracellular and intracellular media is modeled as a resistance and every infinitesimal portion of the membrane is modeled as a capacitance. The circuit analysis allows us to combine all the intracellular resistances, all the extracellular resistances and all the membrane capacitances into a single resistor and capacitors as shown on the right of Figure 4: a resistor, Rn representing the intracellular medium is in series with a capacitor, Cn, which represents the membrane and the branch is in parallel with another resistor, Ricm, which represents the extracellular medium.

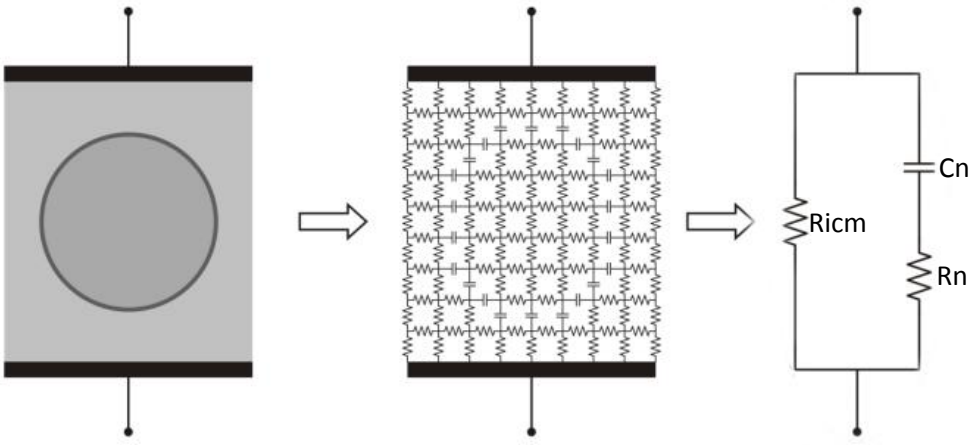

Figure 1. Circuit Model of Liver Cell

This liver cell model, whose impedance is represented as Zlc, forms the building

unit of the liver tissue. The impedance of this liver cell model is calculated as follow:

$$\mathrm{Zlc} = \frac{\mathrm{Ricm} + \mathrm{s} \times \mathrm{Rn} \times \mathrm{Cn} \times \mathrm{Ricm}}{1 + \mathrm{s} \times \mathrm{Cn}(\mathrm{Ricm} + \mathrm{Rn})}$$

The capacitance of Cn is related to the permeability of the cell membrane. Capacitor behaves like an open circuit under low frequency current and as a short circuit under high frequency current. Therefore, only high frequency current can penetrate cell membrane and flow through inside the cell while low frequency current can only flow through the extracellular media as shown in Figure 5.

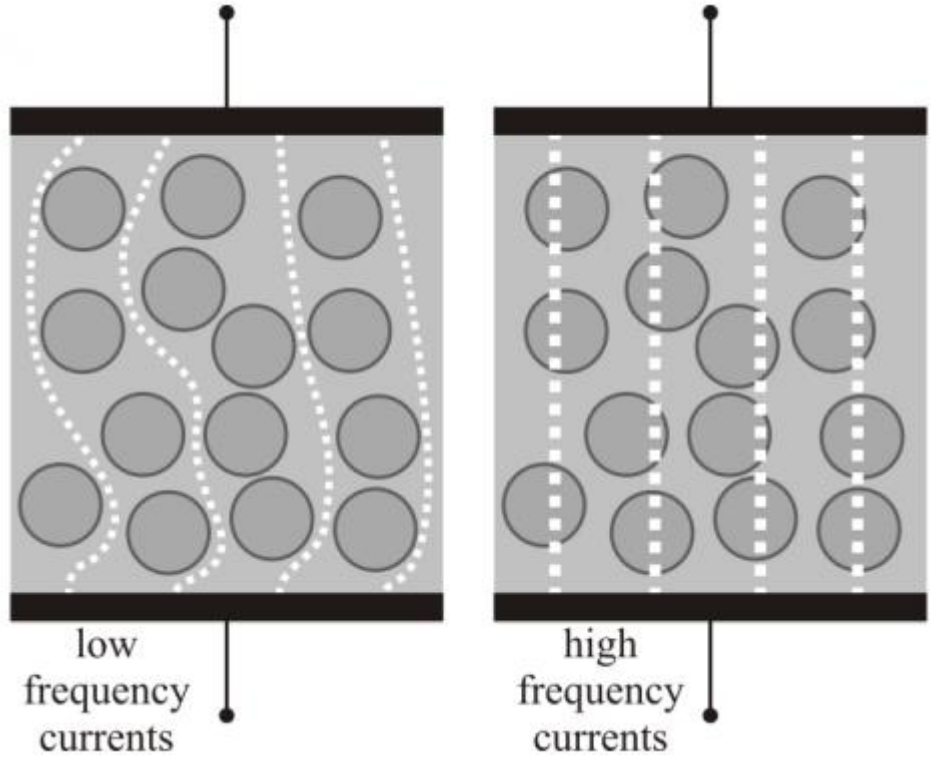

Figure 2. Current Flow through Living Tissue

4.2 Effect of Temperature on Cell

For human body, the normal temperature is around 37 ℃. Our body can sustain a temperature as high as 40 ℃ without suffering from any permanent or structural damage on the cell. However, when the temperature of the cell rises to 50 ℃, cells can die in approximately 6 minutes. If our body temperature reaches 60 ℃, cell death can happen instantaneously. At 60 ℃, the hydrothermal bonds between protein molecules can be broken instantly and reformed when the temperature decreases. This leads to the phenomenon----'Coagulation' that is of interest to surgeons. At temperature between 60 ℃ and 95 ℃ (below 100 ℃), besides the denaturation of protein which is the breaking of hydrothermal bonds, dehydration or desiccation of the cell will also occur. This is because the cell wall is thermally damaged and cell loses its water content. When the cell temperature reaches 100 ℃, the intracellular water will start to boil to form steam. This explosive vaporization of the cell can be as well used by surgeons as it leads to cutting effect through the cell. If the temperature rises even higher to about 200 ℃, carbonization will occur as organic molecules are broken down and tissue will appear to have a brown or black color. (Munro, 2012) The typical effect of cell at different temperatures is summarized in the table below.

Temperature (℃)	Cell Effect
37	Normal
50-60	Cell death in 1 to 6 minutes
60-90	Instant cell death, protein coagulation, cellular desiccation
100	Cellular vaporization
200	Carbonization

Table 1. Cell effect of different temperature

4.3 Effect of Alternating Current on Cell

Radiofrequency energy is delivered to the tissue through RF current which is an alternating current in the range of 100 kHz to 3 MHz. Therefore, to study the effect of alternating current on cell is also important. High frequency alternating current has the capability to increase tissue and cellular temperatures and this happens through three mechanisms. First one is the conversion of electromagnetic energy to mechanical energy which is then converting to thermal energy due to frictions. The second one is resistive heating. This is because current flowing through the tissue with impedance will increase the temperature of the tissue just like current flowing through a resistor. The last and indirect mechanism is

conductive heat transfer. The increase in temperature causes the cells to vaporize and therefore results in a rupture of the tissue. This results in the cutting of the tissue. The heating effect of the RF alternating currents can cauterize the tissue and coagulate the blood. The heating of the tissue is due to the power dissipation in the tissue. (Munro, 2012)

4.4 Liver Anatomy

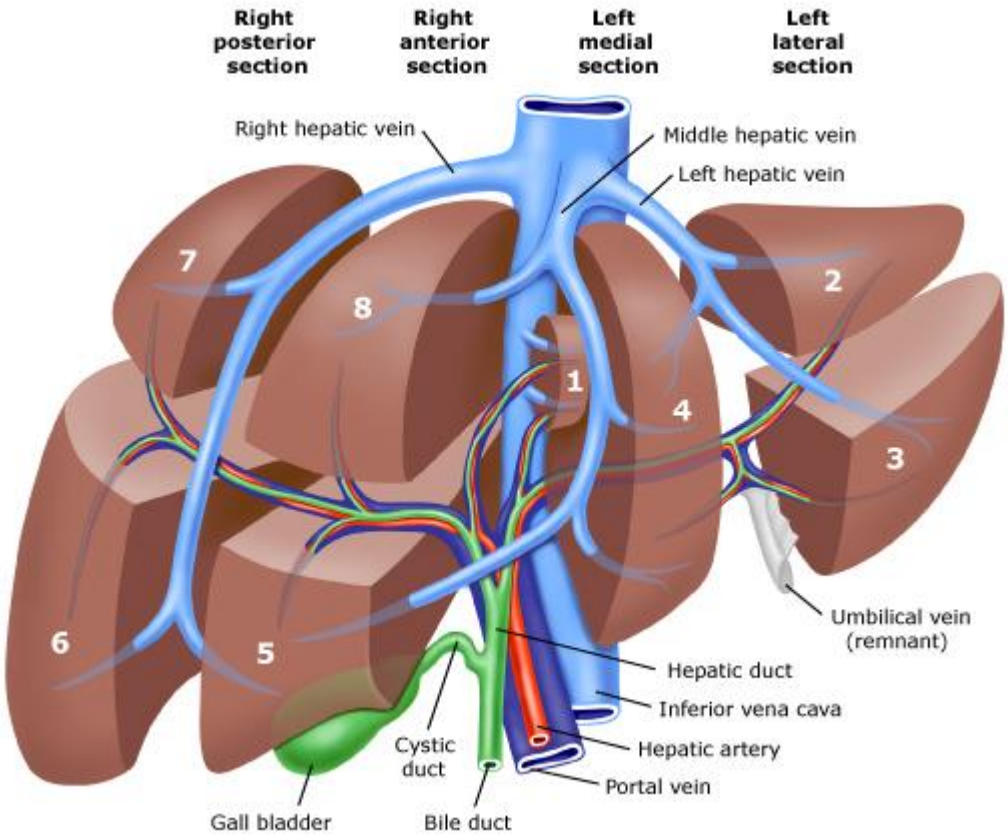

Figure 3. Liver Structure

Liver is human's second largest organ, only after skin and has a wide range of essential functions such as digestion, metabolism, protein synthesis, immunity and

so on. Liver consists of 4 distinct lobes----left, right, caudate, and quadrate lobes, and can be further break down into 8 sections as indicated in Figure 6 above. Besides its own system of arteries which provides oxygenated blood to the liver, liver also has the hepatic portal vein system which makes liver the most vascular organ. Each individual lobule and section has its own unique set of blood vessels. What is also unique about liver is the concept of 'Lobule', so a liver consists of three levels----Liver cell, liver lobule and liver tissue. Each lobule contains some liver cells arranged to form a hexagon and the whole liver is made of approximately 100,000 such lobules. Every lobule has a central vein, which is surrounded by 6 hepatic portal veins and 6 hepatic arteries. Therefore, we use multi-scale circuit model to closely simulate the multi-level nature of liver structure. (Taylor, 1999)

4.5 RF-Assisted Resection Devices in the Market

The currently available radiofrequency-assisted resection devices in the market include: Habib^{TM} 4X bipolar resection device, the Radionics Cool-Tip^{TM} RF Ablation System and the TissueLink Dissecting Sealer. All of them have received marketing approval from the United States Food and Drug Administration (FDA).

4.5.1 Habib™ 4X Bipolar Resection Device

Figure 4. Harbib™ 4X Bipolar Resection Device

The Habib™ 4X bipolar resection device is a bipolar radiofrequency device consisting of a 2x2 array of needles arranged in a rectangle. It is introduced perpendicularly into the liver, along the intended transection line. It produces coagulation of the liver parenchyma by sealing biliary radicals and blood vessels. It enables bloodless transection of the liver parenchyma. (Poon 2007)

4.5.2 Radionics Cool-Tip™ RF Ablation System

Figure 5. Radionics Cool-Top™ RF Ablation System

The Cool-Tip^{TM} RF Ablation System includes generator and electrodes. There is chilled water circulating inside the electrode to cool the adjacent tissue. This unique and internally cooled design can reduce tissue charring and ablation time. (Poon 2007)

4.5.3 TissueLink Dissecting Sealer

Figure 6. TissueLink Dissecting Sealer

In this instrument, saline runs to the tip of the electrode to couple RF energy to the liver surface and achieve coagulation. This device has a pointed tip that allows transection and sealing of vessels simultaneously. TissueLink Dissecting Sealer improves hemostasis during difficult liver resections under cirrhotic conditions. (Boni, Dionigi et al. 2009)

4.6 Electrode-Tissue Interface

Impedance characterization of electrode-tissue interface is essential in simulating the RF-assisted ablation of liver tissue. A few equivalent circuits have been

proposed to model this interface impedance. Warburg first used a polarization resistance in series with a polarization capacitor to represent the interface. (Warburg, 1899) Later experiments and research shows that the value of the polarization capacitor is related to frequency. Therefore, a constant phase angle impedance is used to represent the impedance of the interface capacitance. Nowadays, the well-known Randles' model is commonly used to simulate the electrode-electrolyte interface. Randles' model is shown in Figure 7. (Franks, 2005)

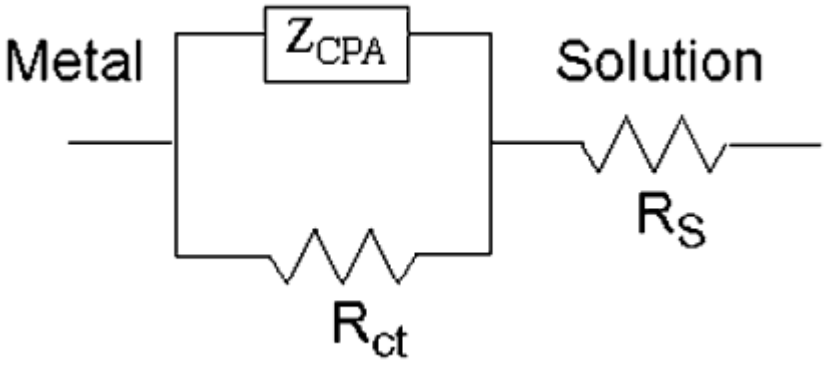

Figure 7. Circuit Model of Electrode

The circuit model consists of a constant phase angle impedance, Z_{CPA}, shunted by a resistor R_{ct}, and another resistor, R_S in series. Z_{CPA} represents interface capacitance impedance, R_{ct} represents the charge transfer resistance and R_S represents solution resistance. This model is adapted from the theoretical models used to simulate the electrode-electrolyte impedance. The impedance equation is represented as follow:

$$Zprobe = \mathrm{Rs} + \frac{\mathrm{Zcpa} \times \mathrm{Rct}}{\mathrm{Zcpa} + \mathrm{Rct}}$$

4.6.1 Interface Capacitance, Z_{CPA}

The constant phase angle impedance, Z_{CPA}, is a measure of the non-faradaic impedance arising from the interface capacitance, or polarization, and is calculated by the following empirical formula (McAdams, 1995):

$$\mathrm{Z_{CPA}}(\omega) = \frac{1}{(\mathrm{j}\omega\mathrm{Q})^{\mathrm{n}}}$$

Where Q is the magnitude of Z_{CPA}, n is a constant ($0 \leq n \leq 1$) which is a measure of inhomogeneities in the surface and w is the angular frequency. When n = 1, Z_{CPA} becomes a purely capacitor which represents the interface capacitance.

4.6.2 Charge Transfer Resistance, R_{ct}

The charge transfer resistance can be calculated experimentally through the following formula:

$$R_{ct} = \frac{\mathrm{RT}}{\mathrm{J_0zF}}$$

which is the slope of the plot of current versus overpotential. RT/F = 26mV at 298K. z is the number of electrons involved in the redox reaction and J_0 is equilibrium exchange current density.

4.6.3 Solution Resistance, R_S

Solution resistance is a measure of resistance between working electrode and

reference electrode. It is the resistance encountered by current spreading out into solution and is referred to as spreading resistance. For typical square electrodes (four electrodes), R_S is calculated as follow:

$$Rs = \frac{\rho \ln 4}{\pi l}$$

where ρ is the solution resistivity and l is the electrode side length (Kovacs, 1994).

4.7 Relationship between Bio-impedance and Temperature

The electrical resistivity in living tissue is related to temperature in two ways: (1) the temperature coefficients of conductivity of the intra- and extracellular electrolytes and (2) temperature-induced fluid volume shifts in the tissue. (Gersing, 1999)

Esrick and McRae studied the effect of hyperthermia on the electrical conductivity of the EMT6 tumor. The study identified the problem related with the usage of Electrical Impedance Tomography (EIT) in tissue temperature measurement. The structural changes in the tissue due to hyperthermia caused the non-thermal conductivity related changes. A method was proposed to identify the start of such structural changes in the tissue by comparing the gradient of the impedance graph with the temperature graph between high frequency impedance (1MHz) and lower frequency impedance (44KHz). The conclusion is that the devised impedance method can only determine the temperature changes but not the actual tissue

temperatures. (Esrick & McRae, 1992)

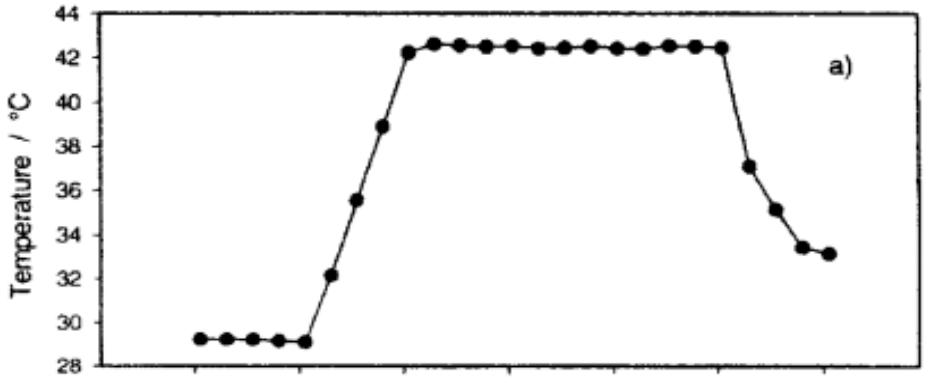

Figure 8. Plot of temperature against time

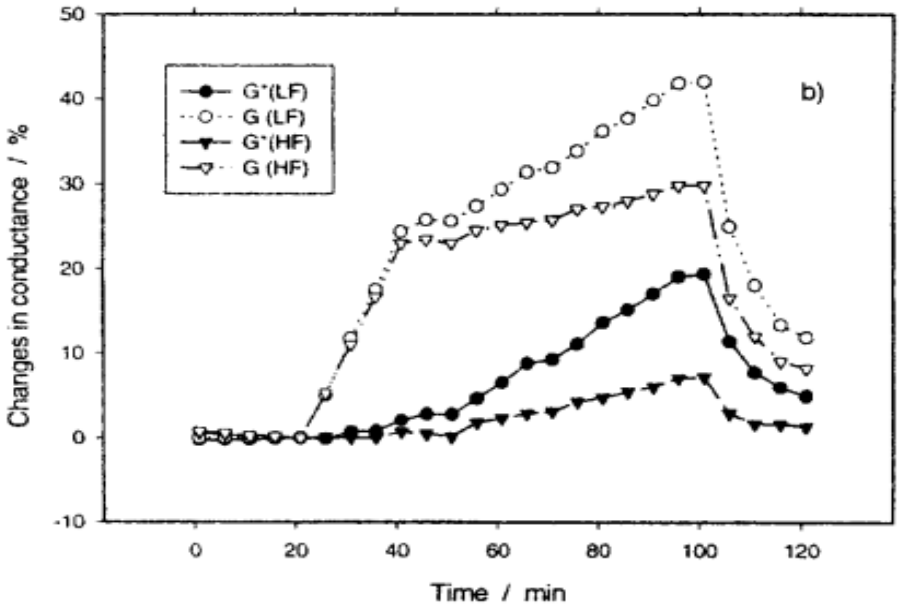

Figure 9. Plot of conductance against time

During the warming-up period, the graph of measured changes in extracellular conductance and the graph of total conductance coincide. During the cooling-down period, the two graphs only coincides partially. The temperature coefficients of total conductance at low frequency and high frequency are

estimated as 1.7%/℃. Initially, there is no change in the residual conductance of the extracellular pathways. Therefore, the increase in the measured conductance is only caused by the temperature coefficients of extracellular and intracellular fluids. This behavior suggested that there is a lack of regulation of blood circulation in tumor vessels. However, 10 minutes after having reached the final temperature of 42.5℃ during the hyperthermic period, a great rise in conductance occurred followed by a great decrease. In this case, conductance rises by approximately 20%. This indicates an increase in fluid in the tissue volume under investigation. (Gersing, 1999)

CHAPTER 5. MULTI-SCALE LIVER MODEL

A multi-scale model is used to study the bio-impedance of liver tissue. Multi-scale model is applicable due to the inherent hierarchical structure of biological tissues. Liver tissue is consisted of liver lobule, which is formed by liver cells. Therefore, there are three levels in our multi-scale model: liver cell, liver lobule and liver tissue. The impedance of each level is derived and combined. A probe model is also proposed to simulate the interface between electrode and electrolyte (liver tissue).

5.1 Cell Model

The building units of the model are liver cells, whose impedance is represented by ZIC. It consists of a resistor, Ricm in parallel with a brand which contains a capacitor, Cn and a resistor, Rn in series. As shown in Figure 10, Ricm represents intracellular matrix, Rn represents the resistance of cell nucleus while Cn represents nucleus membrane. (Huang, 2012) The cell impedance equation derived from the equivalent circuit model is as follow:

$$\mathrm{Zlc} = \frac{\mathrm{Ricm} + \mathrm{s} \times \mathrm{Rn} \times \mathrm{Cn} \times \mathrm{Ricm}}{1 + \mathrm{s} \times \mathrm{Cn}(\mathrm{Ricm} + \mathrm{Rn})}$$

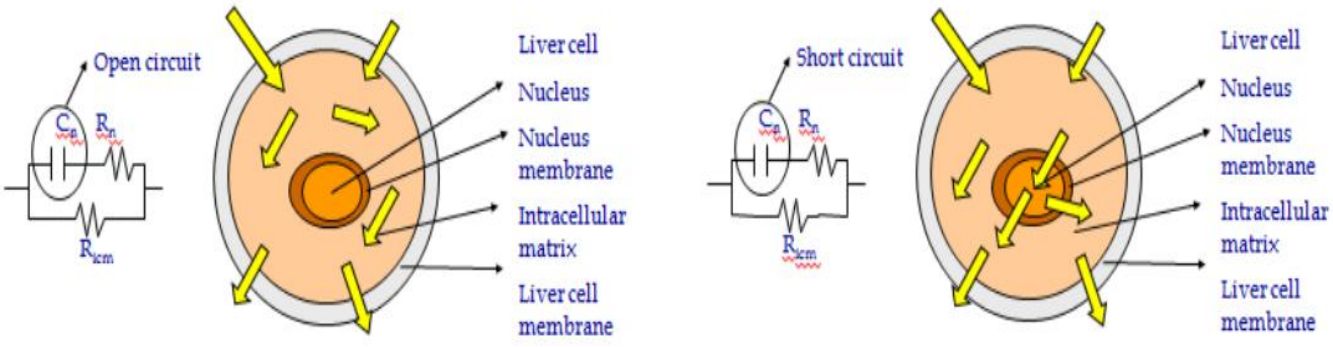

Figure 10. Liver Cell Model under Low Frequency (Left) and High Frequency (Right)

As shown in Figure 10 (Left), capacitor behaves like an open circuit under low frequency. Therefore, current can only flow through intracellular matrix. Under high frequency as shown in Figure 10 (Right), capacitor behaves like a short circuit and hence, current can pass through the nucleus membrane. In this case, current flows through both intracellular matrix and nucleus.

The Bode plot of liver cell impedance is shown in the Figure 3. From the graph, we can see that, at low frequency, the impedance magnitude is equal to Ricm (Cn open circuit), while at high frequency, the impedance magnitude is equal to Ricm//Rn (Cn short circuit). For most biological tissue, the transition from low frequency to high frequency occurs at about 10KHz to 1MHz.(Ivorra 2010)

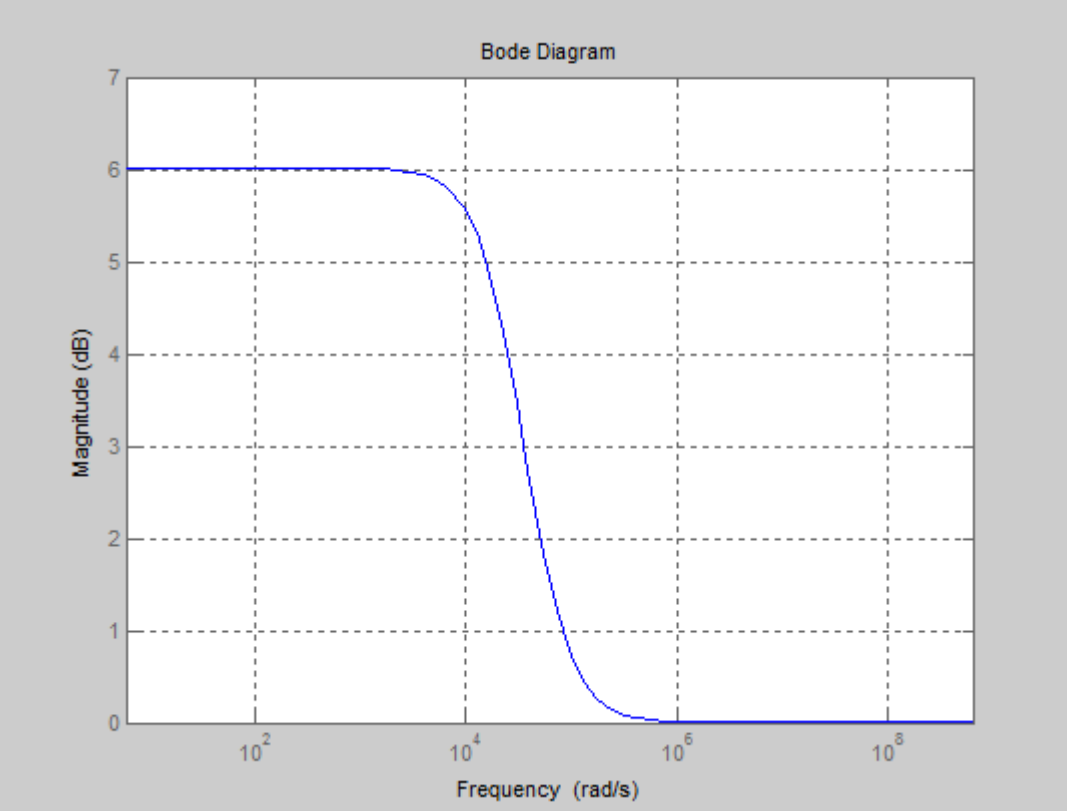

Figure 11. Impedance Magnitude against Frequency of Liver Cell Model

Based on experiment conducted by Pilwat, extracellular medium has a resistivity of 0.66 Ω.m at 37 °C while intracellular medium has a resistivity of 1.66 Ω.m (Pilwat, 1985). The extracellular medium, cell membrane and intracellular medium form a conductor-dielectric-conductor structure and behave as a capacitor. Experimentally, the capacitance has a value of approximately 0.01F/m2 (Ivorra 2010).

5.2 Lobule Model

The next level of the model is liver lobules which consist of liver cells and a central vein which is a micro vessel as shown in Figure 12. At low frequency, the

current cannot pass through the liver lobule membrane and can only flow through the lobule extracellular matrix while high frequency current can pass through the lobule membrane as well as red blood cell membrane and liver cell membrane.

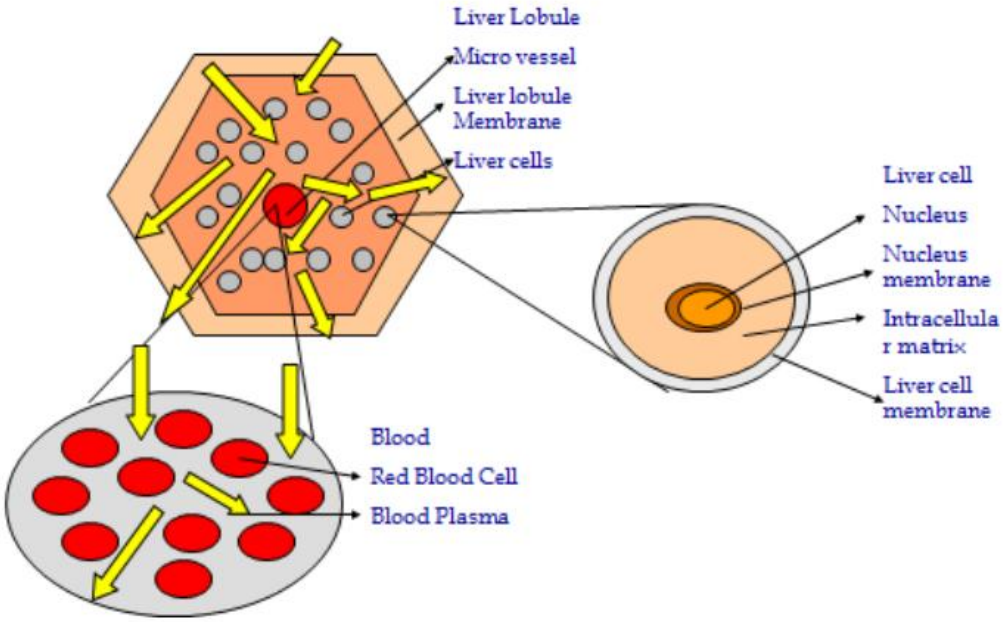

Figure 12. Liver Lobule Model

The micro vessel and liver lobule share a similar structure as the liver cell. As shown in Figure 13, the liver cell model is integrated into the lobule level and N represents the number of liver cells. C_{Ic} represents the liver lobule membrane and R_{lecm} represents the resistance of lobule extracellular medium. For the micro vessel, C_{rbc} represents the capacitance of red blood cell membrane, R_{rbc} represents the resistance of red blood cell while the R_{plasma} represents the resistance of blood plasma.

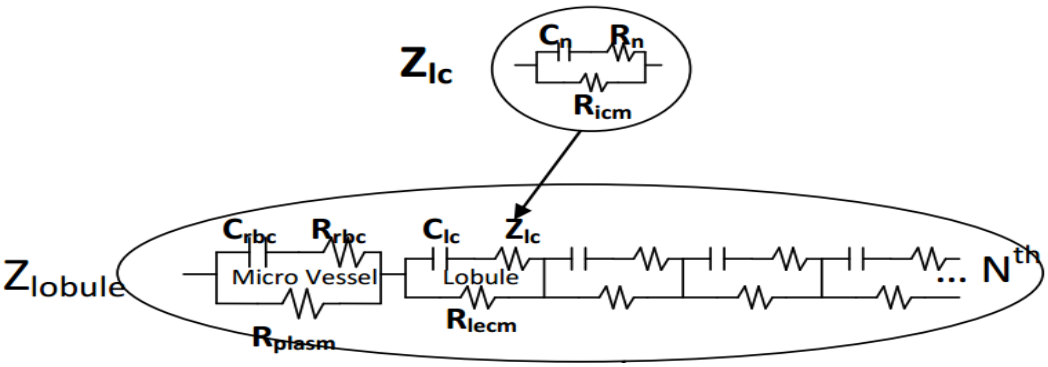

Figure 13. Circuit Model of Liver Lobule

The impedance equations of the micro vessel and lobule are derived as follow:

$$\text{Zmicro vessel} = \text{L}\frac{\text{Rplasma} + \text{s} \times \text{Crbc} \times \text{Rrbc} \times \text{Rplasma}}{1 + \text{s} \times \text{Crbc}(\text{Rrbc} + \text{Rplasma})}$$

$$\text{Zlobule} = \text{Zmv} + \text{N}\frac{\text{Rlecm} + \text{s} \times \text{Clc} \times \text{Zlc} \times \text{Rlecm}}{1 + \text{s} \times \text{Crbc}(\text{Rlecm} + \text{Zlc})}$$

The Bode Plot of liver lobule impedance is shown in Figure 14. At low frequency, the impedance magnitude is equal to R_{plasma} and N R_{lecm} connected in series while at high frequency, the impedance magnitude becomes much lower and is a series combination of Z_{lc} and R_{lecm} in parallel.

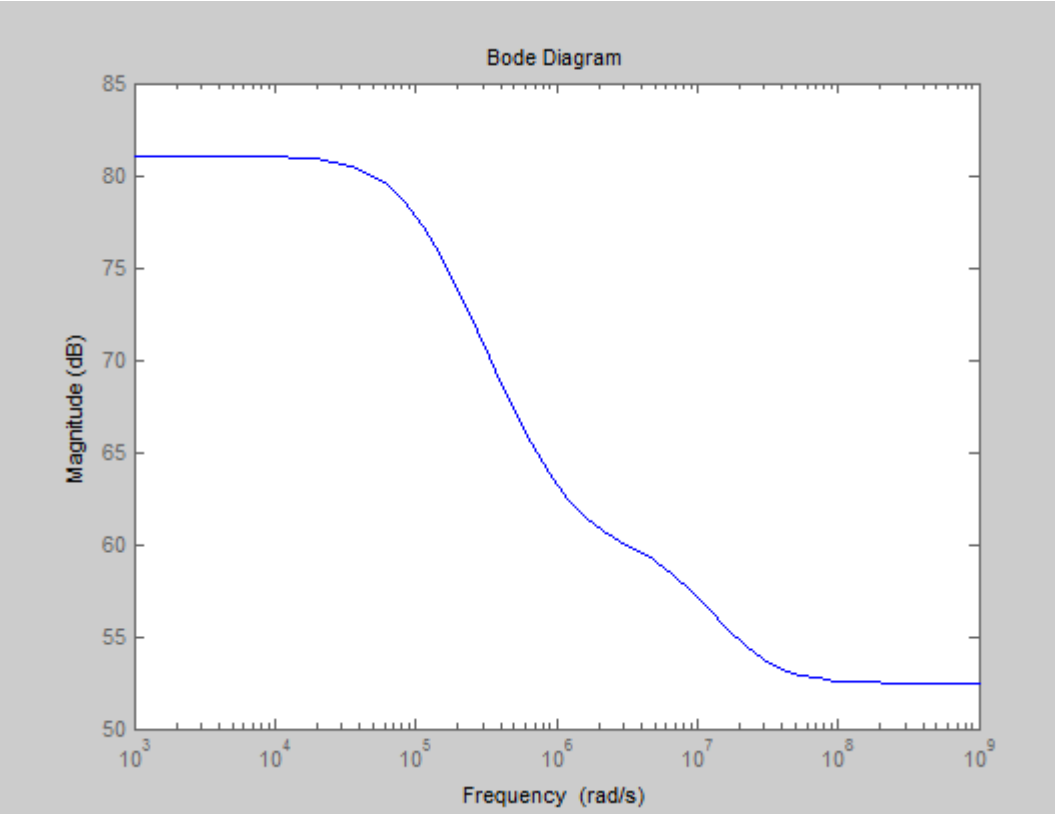

Figure 14. Impedance Magnitude against Frequency of Liver Lobule Model

5.3 Tissue Model

The last level of the model is liver tissue and it consists of liver lobule and a blood vessel. Liver tissue again has a similar structure as liver lobule. The liver tissue model and the current flow under low frequency and high frequency are shown in Figure 15. At low DC/low frequency, all the membranes represented by capacitor behave like open-circuit and thus, electrical current only flows through the plasma and extracellular matrix. As frequency increases, the resistivity becomes more capacitive and at high frequency, the complex resistance becomes the two impedances in parallel.

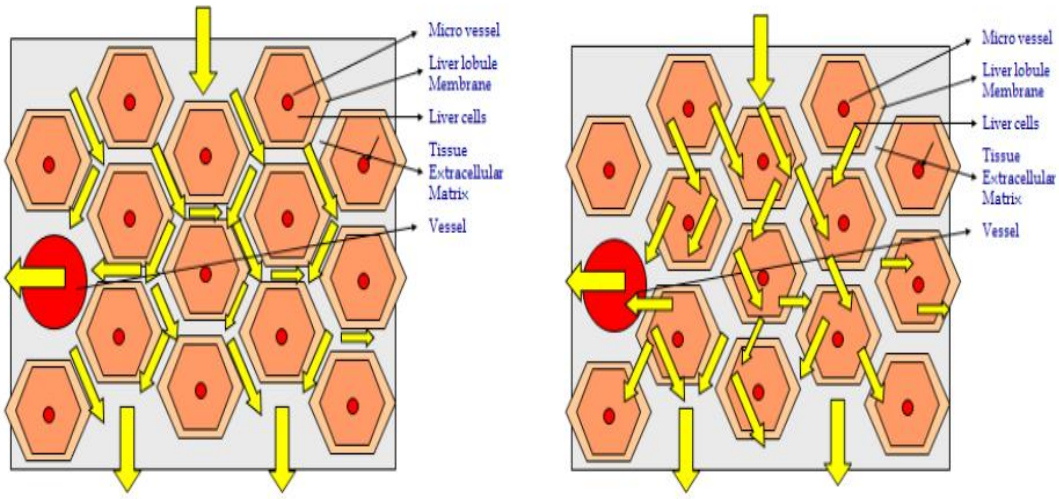

Figure 15. Liver Tissue Model and Low Frequency Current Flow (Left) and High Frequency Current Flow (Right)

The equivalent circuit model of liver tissue is shown in Figure 16 below. M represents the number of liver lobules in liver tissue. The liver lobule circuit model is integrated into the liver tissue model and is represented as Z_{lobule}. C_{lobule} is the capacitance of liver tissue membrane and R_{tecm} represents the resistance of liver tissue extracellular medium. The micro vessels at lobule level merge and become bigger blood vessels at the tissue level but they share the same structure and electrical properties. For the blood vessel, C_{rbc} represents the capacitance of red blood cell membrane, R_{rbc} represents the resistance of red blood cell while the R_{plasm} represents the resistance of blood plasma.

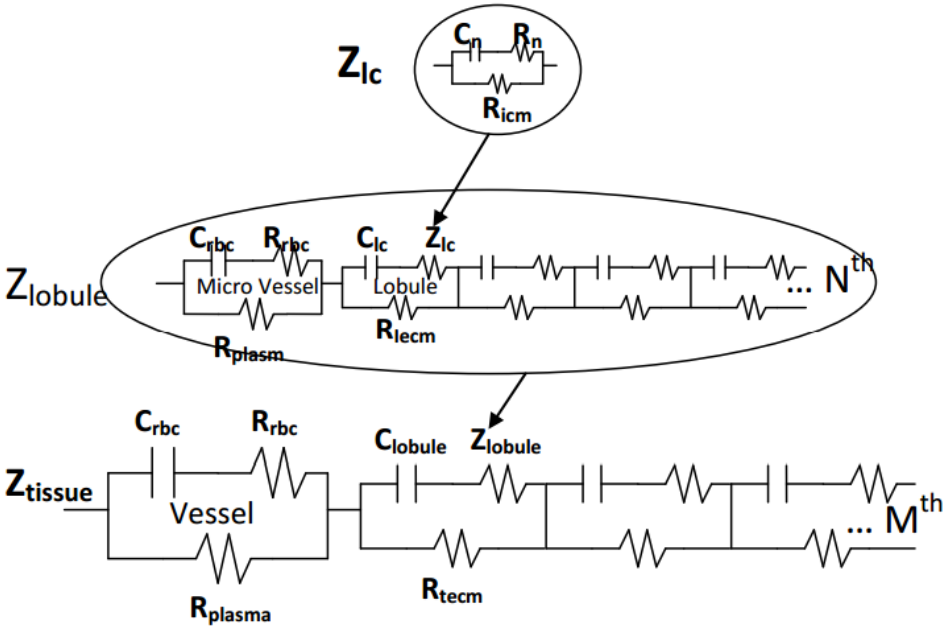

Figure 16. Circuit Model of Liver Tissue

The impedance equations of the blood vessel and liver tissue are derived as follow:

$$\text{Zvessel} = \text{K}\frac{\text{Rplasma} + \text{s} \times \text{Crbc} \times \text{Rrbc} \times \text{Rplasma}}{1 + \text{s} \times \text{Crbc}(\text{Rrbc} + \text{Rplasma})}$$

$$\text{Ztissue} = \text{Zvessel} + \text{M}\frac{\text{Rtecm} + \text{s} \times \text{Clobule} \times \text{Zlobule} \times \text{Rtecm}}{1 + \text{s} \times \text{Clobule}(\text{Rtecm} + \text{Zlobule}}$$

The Bode Plot of liver tissue impedance is shown in Figure 17 below.

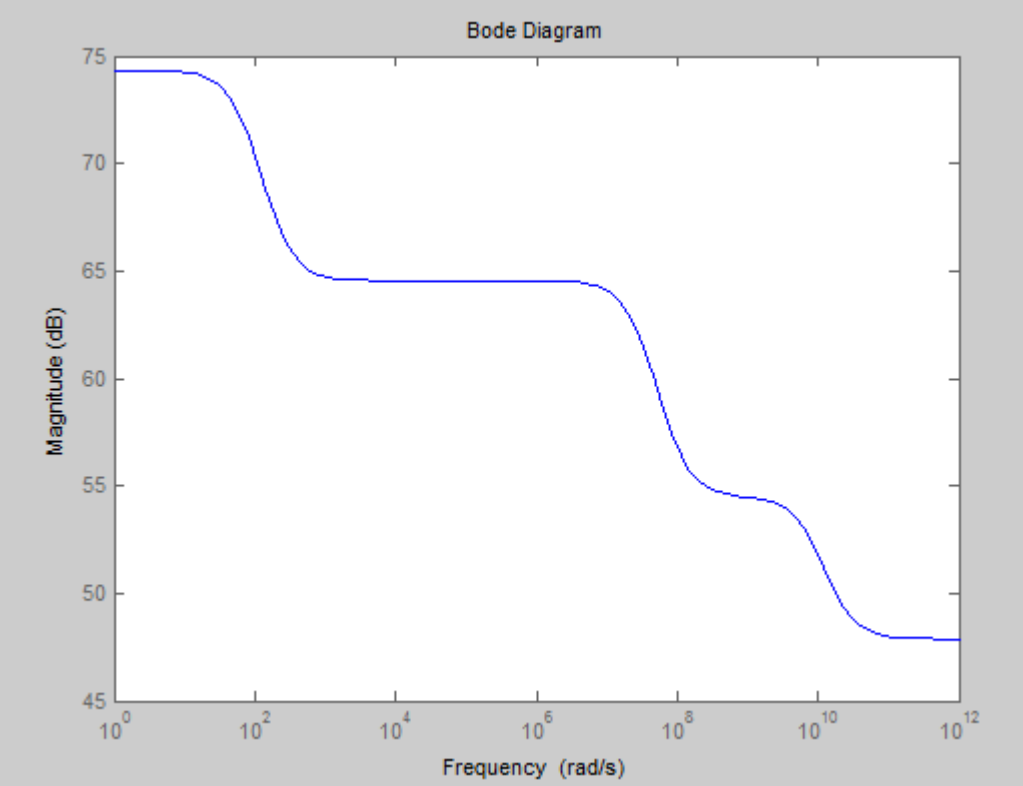

Figure 17. Impedance Magnitude against Frequency of Liver Tissue Model

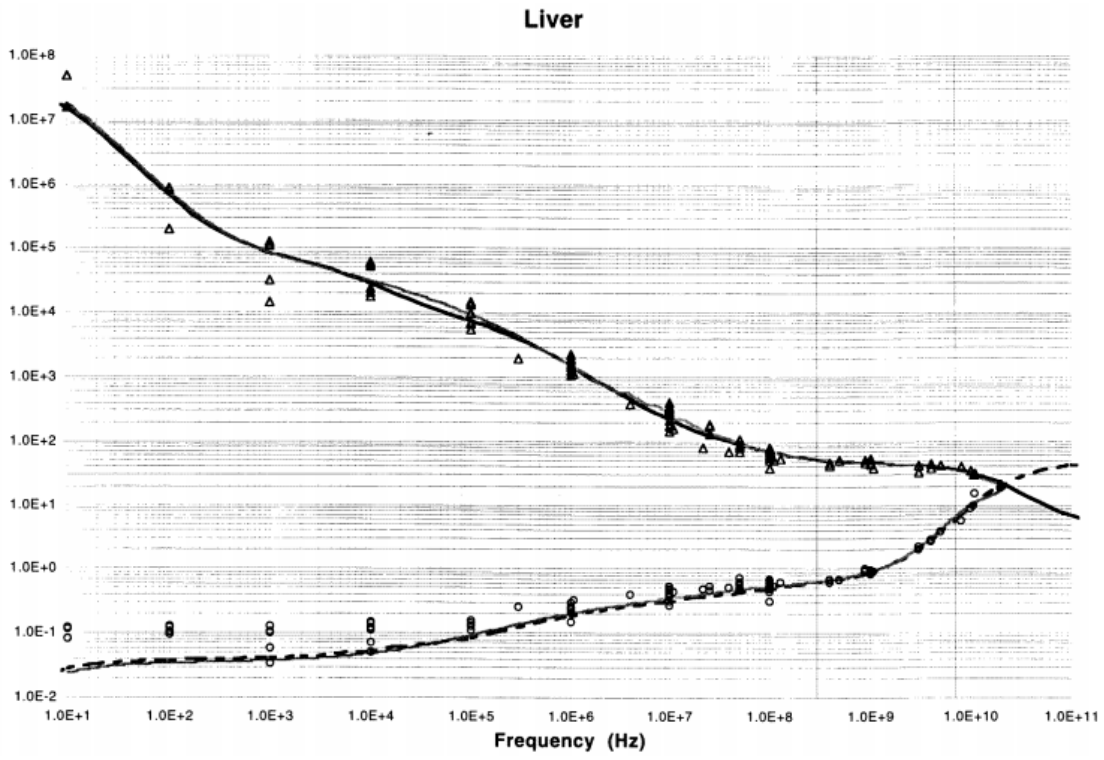

Figure 18. Liver permittivity and conductivity against frequency

In 1996, S. Gabriel and his colleagues measured the dielectric properties of various human and animal tissues including liver tissue using three different techniques based on swept-frequency network and impedance analyzers. The experimental results of liver tissue are shown in Figure 18, represented by the small triangles. The graph was obtained through a parametric modeling which displays a high degree of consistency with the experimental results. (Gabriel et al, 1996) The graph on top of Figure 18 is permittivity against frequency while the graph on the bottom is conductivity again frequency. Our simulation graph in Figure 17 is impedance against frequency and our shape of our impedance graph is the mirror image of the permittivity graph obtained by Gabriel. This is because conductivity is the reciprocal of resistivity and thus the impedance. Therefore, when conductance increases, impedance will decrease. The three 'knee points' of the two graph also coincide at approximately the same frequencies. The simulation results show that the multi-scale model can accurately estimate the electrical properties (impedance) of the liver tissue.

5.4 Electrode Model

The model will only be complete until we include the model of a probe (electrode) which model the electrical characteristic of the electrode-electrolyte (liver tissue) interface. The electrode model is also essential in deriving the transfer function of the overall system or model. In order to simulate the electrode-tissue interface,

Randles' model is used.

The circuit model consists of a constant phase angle impedance, Z_{CPA}, shunted by a resistor R_{ct}, and another resistor, R_S in series. Z_{CPA} represents interface capacitance impedance, R_{ct} represents the charge transfer resistance and R_S represents solution resistance. This model is adapted from the theoretical models used to simulate the electrode-electrolyte impedance. The impedance equation is represented as follow:

$$\mathrm{Zprobe} = \mathrm{Rs} + \frac{\mathrm{Zcpa} \times \mathrm{Rct}}{\mathrm{Zcpa} + \mathrm{Rct}}$$

Table 2 below is a summary of the average and fitted parameter results with corresponding standard deviations. For the following materials, the measurement areas for Pt, Pt black, TiN, PLL, Laminin and Neuron Medium are 1 cm^2, the measurement area for electrode Pt black 900 um^2 (Franks, 2005).

	Q $[s\Omega^{-1/n}]$	n	R_s $[\Omega]$	R_{ct} $[\Omega]$
Pt	$2.72(10)^{-5}$	0.92	28.0	$4.48(10)^{5}$
Std. dev.	$0.26(10)^{-5}$	0.01	2.81	$0.88(10)^{5}$
Pt black	$2.08(10)^{-3}$	0.91	30.7	$5.11(10)^{4}$
Std. dev.	$0.11(10)^{-3}$	0.03	7.85	$2.88(10)^{4}$
TiN	$2.03(10)^{-3}$	0.91	42.3	$3.00(10)^{5}$
Std. dev.	$5.77(10)^{-5}$	0.00	3.70	$3.20(10)^{5}$
µelectrode Pt black	$0.86(10)^{-9}$	0.86	$7.38(10)^{3}$	$2.70(10)^{9}$
Std. dev.	$0.52(10)^{-9}$	0.02	$1.74(10)^{3}$	$1.31(10)^{9}$
PLL	$8.57(10)^{-6}$	0.91	37.0	$1.24(10)^{6}$
Std. dev.	$0.51(10)^{-6}$	0.01	2.41	$0.69(10)^{6}$
Laminin	$5.00(10)^{-6}$	0.89	28.3	$2.46(10)^{5}$
Std. dev.	$2.88(10)^{-6}$	0.01	5.64	$0.68(10)^{5}$
Neuron Medium	$1.46(10)^{-5}$	0.91	40.4	$4.26(10)^{5}$
Std. dev.	$0.18(10)^{-5}$	0.01	2.30	$0.57(10)^{5}$

Table 2. Q, Rs and Rct values for different materials

Based on the table above and the Z_{CPA} formula discussed in the literature review, the impedance of the probe is calculated as follow:

$$\text{Zprobe} = \text{Rs} + \frac{\text{Rct}}{1 + \text{Rct}(\text{sQ})^{\text{n}}}$$

Assuming a pure capacitance (n=1) and using TiN as an example, the impedance of the probe is expressed as follow:

$$\text{Zprobe} = 42.3 + \frac{3 * 10\text{^}5}{1 + 609\text{s}}$$

5.5 Results and Discussion

For the above cell impedance, lobule impedance, tissue impedance and probe impedance, the values that are used for the variables in the equations are shown in

Table 3 below.

R_{icm}	450	**M**	0.4	**C_{lobule}**	800*10^-9
R_n	600	**C_{lc}**	0.3*10^-9	**R_{tecm}**	12500
C_n	10^-10	**R_{lecm}**	35000	**R_s**	42.3
L	0.4	**R_{plasma}**	2000	**Q**	2.03*10^-3
N	0.3	**R_{rbc}**	1500	**R_{ct}**	3*10^5
K	0.1	**C_{rbc}**	0.035*10^-9		

Table 3. Parameter values of liver tissue model

These values are obtained through a model fitting algorithm based on the experiment data of Gabriel in 1996 and compared with Cole-Cole Equations. It was done by a PhD using MATLAB (Huang, 2012).

In order to better fit the graph with the experimental results obtained by Gabriel in 1996, some of the above parameter values are adjusted manually and the final values are as shown in Table 4 below.

R_{icm}	450	**M**	0.4	**C_{lobule}**	8*10^-7
R_n	600	**C_{lc}**	3*10^-12	**R_{tecm}**	12500
C_n	10^-10	**R_{lecm}**	15000	**R_s**	42.3
L	0.4	**R_{plasma}**	2000	**Q**	2.03*10^-3
N	0.3	**R_{rbc}**	1500	**R_{ct}**	3*10^5
K	0.1	**C_{rbc}**	3.5*10^-14		

Table 4. Parameter values of liver tissue model after minor adjustment

The transfer function is as follow:

$$H(s) = \frac{Ztissue}{Zprobe + Ztissue}$$

The Bode plot in the frequency domain based on the above values and transfer function are shown below in Figure 19. It behaves like a high pass filter. This is because high frequency current can pass through the membrane while the low frequency or DC current is attenuated. The cut-off frequency is about 0.1 rad/s, which is 0.016 Hz.

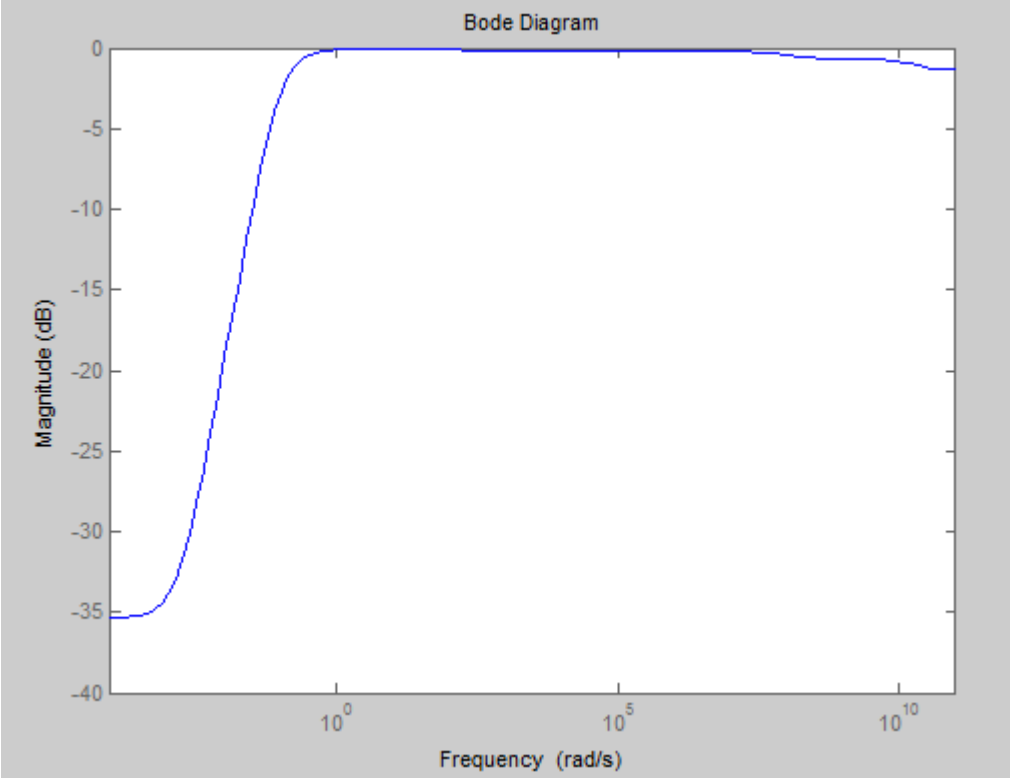

Figure 19. Bode Plot of the Model Transfer Function

CHAPTER 6. SIMULATION SOFTWARE

A simulation software is developed using MATLAB GUI to provide a clear and easy-to-manage program and to better visualize the simulation results. It will also be easier for others to continue on the research topic.

The simulation software is divided into five sections: Cell, Lobule, Tissue, Electrode and System. Figure 20 shows the ‘Cell’ section of the simulation software. The cell model is shown on the bottom right and the impedance equation derived from the cell model is shown on the middle right. After user inputs the three cell parameters and clicks the run, the simulation graph will show on the left.

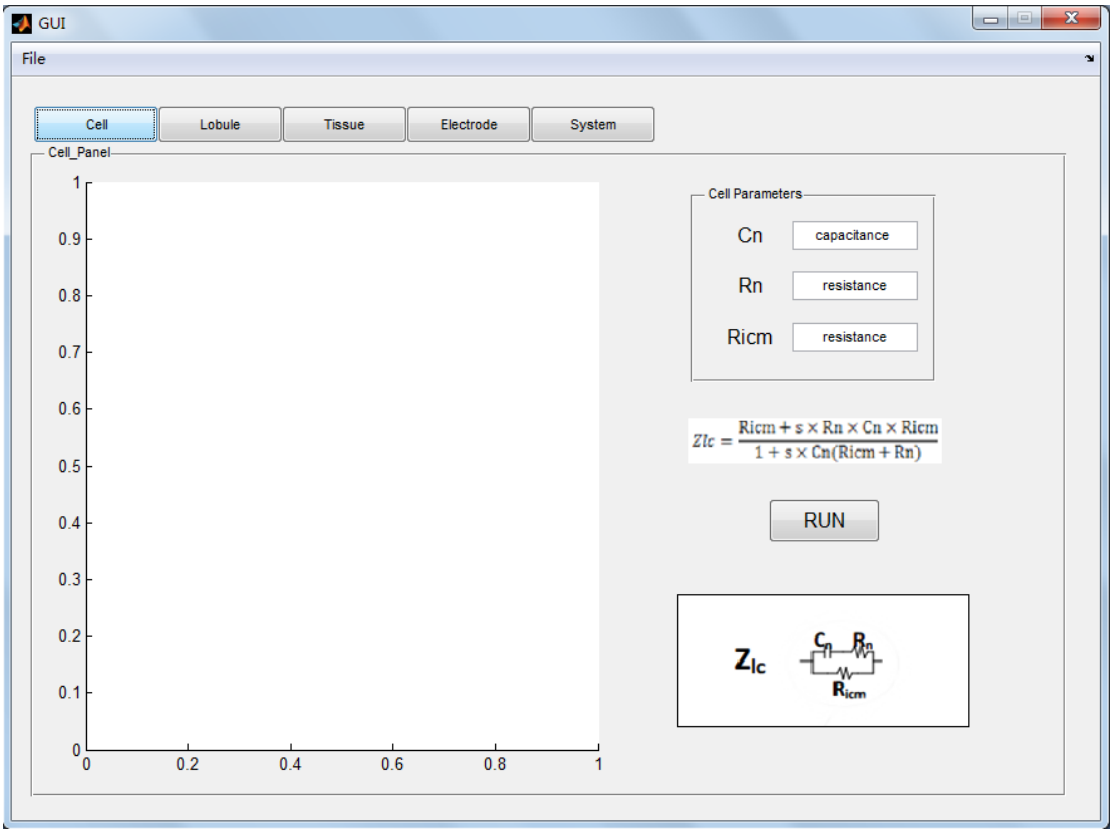

Figure 20. Simulation Software – Cell Tab

The ‘Lobule’ section of the simulation software is shown in Figure 21. On the lobule level, there are liver lobules as well as micro vessels. Therefore, there are two different panels for the two sets of parameters and their respective impedance equations are shown on the middle right. The use of this section of the program is the same as that of the ‘Cell’ section. The cell parameters on the cell sections must be filled before the simulation of liver lobule can be shown correctly. The rest of the program has similar layout and usage as that of the “Cell’ and ‘Lobule’ sections. The screenshots of the ‘Tissue’ tab, ‘Electrode’ tab and ‘System’ tab are shown in Appendix A. The source code of the simulation software is revealed in Appendix B.

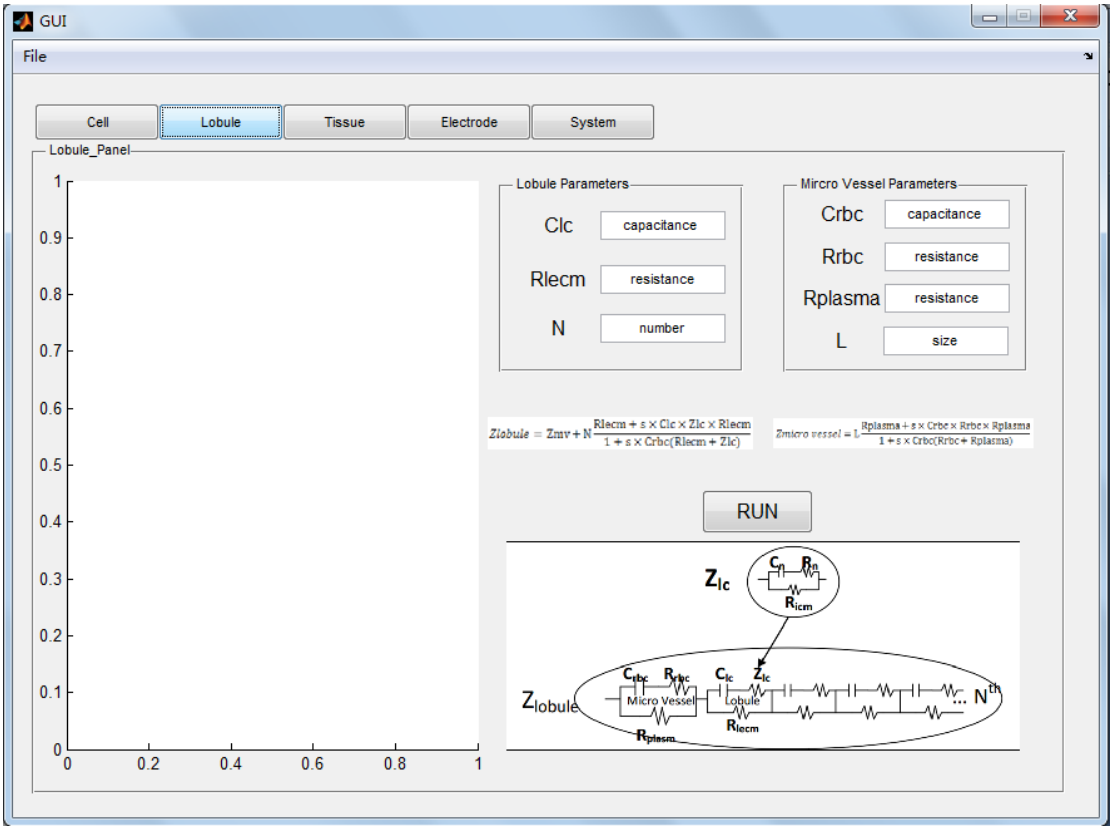

Figure 21. Simulation Software – Lobule Tab

CHAPTER 7. CONCLUSION

7.1 Future Works

There are a lot of parameters involved in our multi-scale liver model, such as intracellular and extracellular resistances and membrane capacitance. With the exact parameter values, the behavior of liver tissue under radiofrequency can be predicted with a high degree of accuracy thus determining the optimal amount of RF energy to supply. Currently, the parameter values are obtained through a data fitting algorithm and adjusted by comparing the simulation graph with the model proposed by Gabriel in 1996. Although the simulation results follows the experiment data obtained by Gabriel and the impedance change is observed at certain frequencies, the exact values of the impedance at each frequency are not verified. Therefore, the exact values of these parameters remain to be examined. Experiments on the porcine liver may be conducted to measure these parameters values and by inputting these values into the simulation software, more insights regarding the behavior of liver tissue under RF energy can be obtained.

It was mentioned earlier that cell death occurs at approximately 60 ℃ and is not directly linked to the bio-impedance. Although various relationships between bio-impedance and temperature have been identified and examined, the exact equation linking impedance to the temperature has yet been confirmed. Bio-impedance can provide some insights on the temperature change of tissue but

not the actual tissue temperatures. (Esrick & McRae, 1999) By finding the exact relationship between bio-impedance and tissue temperature, cell death can be predicted or avoided precisely.

7.2 Conclusion

Radio-frequency energy is commonly deployed to coagulate liver tissue during liver resection. However, blood loss is a major concern during the surgery as liver is very vascular. The optimal amount of RF energy is difficult to be estimated. If more than enough RF energy is applied, unnecessary liver damage will occur. If less than necessary RF energy is applied, there will be bleeding of liver and thus increasing risk for postoperative complications. A multi-scale liver model is proposed to simulate the electrical behavior, especially bio-impedance of liver tissue under RF-energy. A simulation software is also introduced to visualize the simulation results. The multi-scale model is a more complete representation of liver as it incorporates the lobule level and concepts of blood vessels. By understanding the electrical properties (bio-impedance) of liver tissue through the multi-scale model, some insights regarding the temperature change of liver cells and thus the optimal amount of RF energy applied can be obtained.

REFERENCE

Boni, L., et al. (2009). Transection Techniques in Liver Surgery. R. Dionigi, Landes Bioscience.

Chang S KY, Hlaing WW, Huang WH, Chui CK, 2011. Integrated ablation and division device for liver resection. HPB, 13(3).

Chouillard, E. K., et al. (2010). "Vascular clamping in liver surgery: physiology, indications and techniques." Ann Surg Innov Res **4**: 2.

Eberhard Gersing (1999). "Monitoring Temperature-Induced Changes in Tissue during Hyperthermia by Impedance Methods". Annals New York Academy of Sciences

Esrick MA and McRae DA, 1992. The effect of hyperthermia-induced tissue conductivity changes on electrical impedance temperature mapping. Phys. Med. Biol. 39, 133-144

E. T. McAdams, A. Lackermeier, J. A. McLaughlin, D. Macken, and J. Jossinet, "The linear and nonlinear electrical properties of the electrodeelectrolyte interface," Biosensors Bioelectron., vol. 10, pp. 67–74, 1995.

E. Warburg, "Ueber das Verhalten sogenannter unpolarisbarer Elektroden gegen Wechselstrom," Annalen der Physik und Chemie, vol. 67, pp. 493–499, 1899

Franks, W., et al. (2005). "Impedance Characterization and Modeling of Electrodes for Biomedical Applications." IEEE TRANSACTIONS ON BIOMEDICAL ENGINEERING **52**(7): 8.

Gabriel S, Lau RW, Gabriel C,1996. The Dielectric properties of biological tissues: III. Parametric models for the dielectric spectrum of tissues. Phys. Med. Biol. , 41, 2271 - 2293.

G. Pilwat and U. Zimmermann, "Determination of intracellular conductivity from electrical breakdown measurements," Biochimica et Biophysica Acta, vol. 820, pp. 305- 314, 1985.

G. T. A. Kovacs, “Introduction to the theory, design, and modeling of thin-film microelectrodes for neural interfaces,” in Enabling Technologies for Cultured Neural Networks, D. A. Stenger and T. M. McKenna, Eds. London, U.K.: Academic, 1994, pp. 121–165.

H. Fricke, "A mathematical treatment of the electric conductivity and capacity of disperse systems. II. The capacity of a suspension of conducting spheroids surrounded by a nonconducting membrane for a current of low frequency," Physical Review, vol. 26, 1925.

Huang, W. H., et al. (2012). "A Multiscale Model for Bioimpedance Dispersion of Liver Tissue." IEEE TRANSACTIONS ON BIOMEDICAL ENGINEERING **59**(6): 5.

Ivorra, A. (2010). Tissue electroporation as a bioelectric phenomenon: basic concepts, Springer Berlin Heidelberg.

Malcolm.G.Munro (2012). Fundamentals of Electrosurgery. Part I: Principles of Radiofrequency Energy for Surgery. L.S. Feldman et al. (eds.), The SAGES Manual on the Fundamental 15 Use of Surgical Energy (FUSE), DOI 10.1007/978-1-4614-2074-3_2,

Poon, R. T. (2007). "Current techniques of liver transection." HPB (Oxford) **9**(3): 166-173.

SingHealth (2014). "Conditions & Treatments " Liver Cancer. from http://www.singhealth.com.sg/PatientCare/ConditionsAndTreatments/Pages/liver-Cancer.aspx.

Tim Taylor (1999), Anatomy of the Liver. INNERBODY.COM from http://www.innerbody.com/image_digeov/card10-new2.html

APPENDIX A

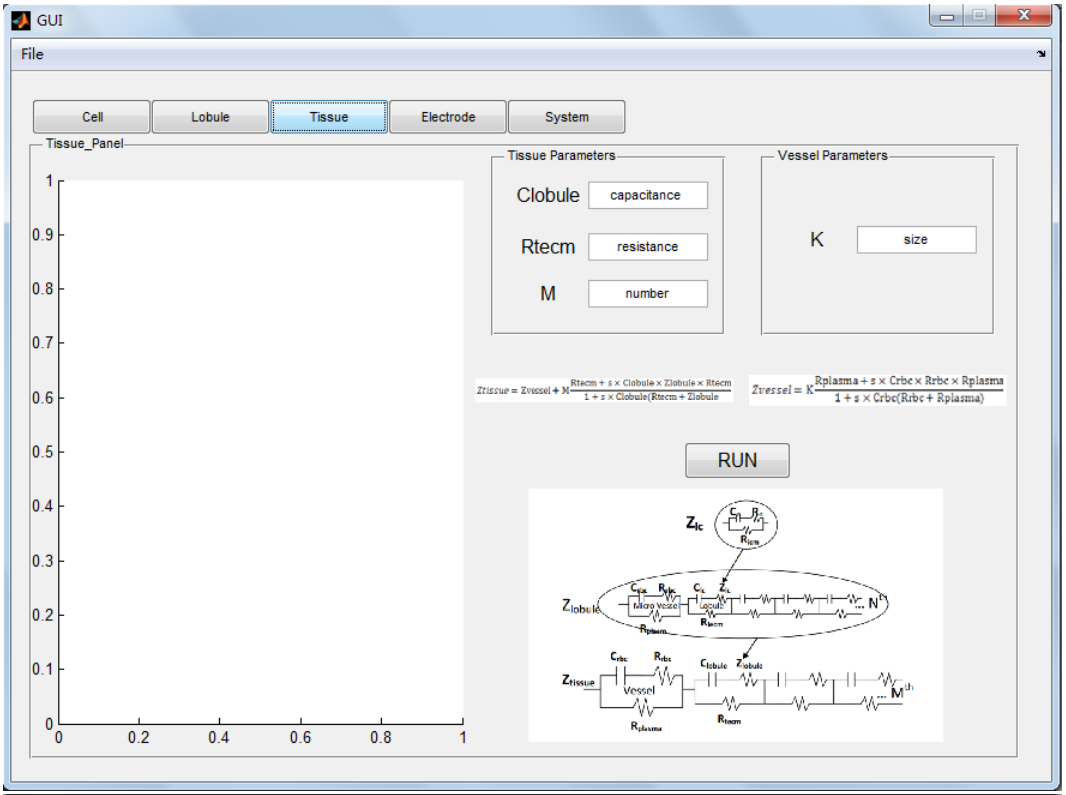
GUI
File
Cell
Lobule
Tissue
Electrode
System
Tissue_Panel
Tissue Parameters
Clobule
capacitance
Rtecm
resistance
M
number
Vessel Parameters
K
size
RUN

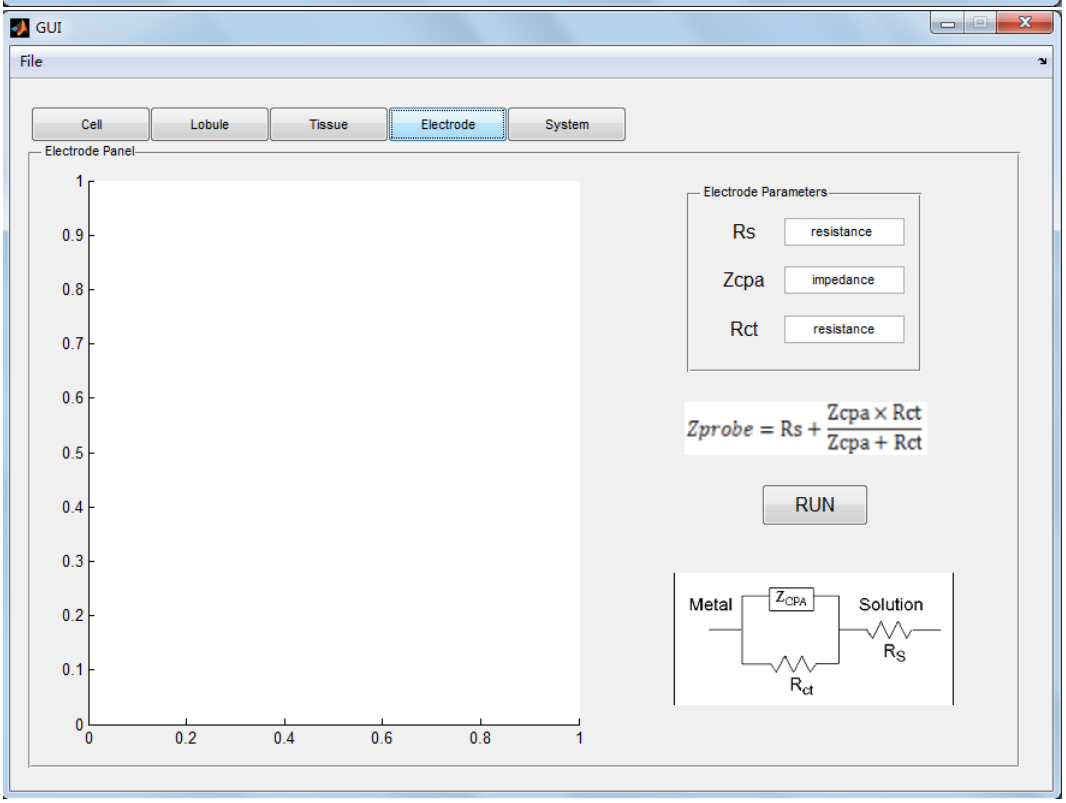
GUI
File
Cell
Lobule
Tissue
Electrode
System
Electrode Panel
Electrode Parameters
Rs
resistance
Zcpa
impedance
Rct
resistance
RUN
Metal
Solution

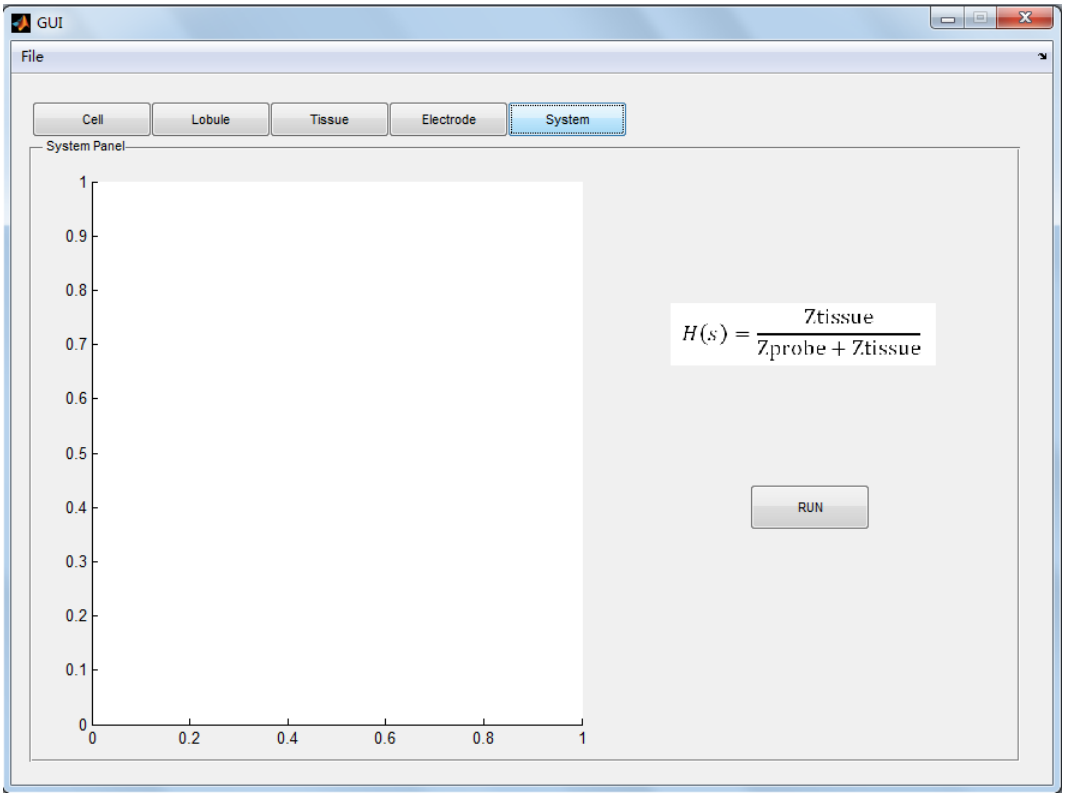
GUI
File
Cell
Lobule
Tissue
Electrode
System
System Panel
1
0.9
0.8
0.7
0.6
0.5
0.4
0.3
0.2
0.1
0
0
0.2
0.4
0.6
0.8
1
$H(s) = \frac{Ztissue}{Zprobe + Ztissue}$
RUN

APPENDIX B

```
function varargout = GUI(varargin)

%initialisation
gui_Singleton = 1;
gui_State = struct('gui_Name',           mfilename, ...
                   'gui_Singleton',    gui_Singleton, ...
                   'gui_OpeningFcn', @GUI_OpeningFcn, ...
                   'gui_OutputFcn',    @GUI_OutputFcn, ...
                   'gui_LayoutFcn',    [] , ...
                   'gui_Callback',     []);
if nargin && ischar(varargin{1})
    gui_State.gui_Callback = str2func(varargin{1});
end

if nargout
    [varargout{1:nargout}] = gui_mainfcn(gui_State, varargin{:});
else
    gui_mainfcn(gui_State, varargin{:});
end
% End initialization

% --- Executes just before GUI is made visible.
function GUI_OpeningFcn(hObject, eventdata, handles, varargin)
handles.output = hObject;
% Update handles structure
guidata(hObject, handles);
% only cell tab is visible on launch of the program
set (handles.Cell_Panel, 'Visible', 'on' );
set (handles.Tissue_Panel, 'Visible', 'off' );
set (handles.Lobule_Panel, 'Visible', 'off' );
set (handles.Electrode_Panel, 'Visible', 'off' );
set (handles.System_Panel, 'Visible', 'off' );
%load cell model and equation
axes(handles.model);
imshow('Cell.png');
axes(handles.equation);
imshow('Cell_Eq.png');

function varargout = GUI_OutputFcn(hObject, eventdata, handles)
varargout{1} = handles.output;
% --- Executes on button press in Cell.
```

```
function Cell_Callback(hObject, eventdata, handles)
% only cell panel is visible when button is pressed
set (handles.Cell_Panel, 'Visible', 'on' );
set (handles.Tissue_Panel, 'Visible', 'off' );
set (handles.Lobule_Panel, 'Visible', 'off' );
set (handles.Electrode_Panel, 'Visible', 'off' );
set (handles.System_Panel, 'Visible', 'off' );
%load cell model and equation
axes(handles.model);
imshow('Cell.png');
axes(handles.equation);
imshow('Cell_Eq.png');

% --- Executes on button press in Lobule.
function Lobule_Callback(hObject, eventdata, handles)
%only lobule panel is visible when button is pressed
set (handles.Lobule_Panel, 'Visible', 'on' );
set (handles.Cell_Panel, 'Visible', 'off' );
set (handles.Tissue_Panel, 'Visible', 'off' );
set (handles.Electrode_Panel, 'Visible', 'off' );
set (handles.System_Panel, 'Visible', 'off' );
%load lobule model and equation
axes(handles.lobule_mod);
imshow('Lobule.png');
axes(handles.lobule_eq);
imshow('Lobule_Eq.png');
axes(handles.micro_vessel_eq);
imshow('Micro_Vessel_Eq.png');

% --- Executes on button press in Tissue.
function Tissue_Callback(hObject, eventdata, handles)
% only tissue panel is visible when button is pressed
set (handles.Tissue_Panel, 'Visible', 'on' );
set (handles.Cell_Panel, 'Visible', 'off' );
set (handles.Lobule_Panel, 'Visible', 'off' );
set(handles.Electrode_Panel, 'Visible', 'off');
set (handles.System_Panel, 'Visible', 'off' );
%load tissue model and equation
axes(handles.tissue_mod);
imshow('Tissue.png');
axes(handles.vessel_eq);
imshow('Vessel_Eq.png');
axes(handles.tissue_eq);
```

```
imshow('Tissue_Eq.png');

% --- Executes on button press in Electrode.
function Electrode_Callback(hObject, eventdata, handles)
% only electrode panel is visible when the button is pressed
set (handles.Electrode_Panel, 'Visible', 'on');
set (handles.Tissue_Panel, 'Visible', 'off' );
set (handles.Cell_Panel, 'Visible', 'off' );
set (handles.Lobule_Panel, 'Visible', 'off' );
set (handles.System_Panel, 'Visible', 'off' );
%load electrode model and equation
axes(handles.electrode_mod);
imshow('Electrode.png');
axes(handles.electrode_eq);
imshow('Electrode_Eq.png');

% --- Executes on button press in System.
function System_Callback(hObject, eventdata, handles)
%only system panel is visible when the button is pressed
set (handles.Electrode_Panel, 'Visible', 'off');
set (handles.Tissue_Panel, 'Visible', 'off' );
set (handles.Cell_Panel, 'Visible', 'off' );
set (handles.Lobule_Panel, 'Visible', 'off' );
set (handles.System_Panel, 'Visible', 'on' );
%load system equation
axes(handles.system_eq);
imshow('System_Eq.png');

% --- Executes on button press in run.
function run_Callback(hObject, eventdata, handles)
% read data from the field and sub into equation
s = tf('s');
Cn = str2double(get(handles.Cn, 'String'));
Rn = str2double(get(handles.Rn, 'String'));
Ricm = str2double(get(handles.Ricm, 'String'));
Zlc = (Ricm+s*Ricm*Cn*Rn)/(1+s*Cn*(Rn+Ricm));
%plot graph
axes(handles.simulation);
bode(Zlc);

% --- Executes during object creation, after setting all properties.
function Cn_CreateFcn(hObject, eventdata, handles)
if ispc && isequal(get(hObject,'BackgroundColor'),
get(0,'defaultUicontrolBackgroundColor'))
```

```
    set(hObject,'BackgroundColor','white');
end

% --- Executes during object creation, after setting all properties.
function Rn_CreateFcn(hObject, eventdata, handles)
if ispc && isequal(get(hObject,'BackgroundColor'),
get(0,'defaultUicontrolBackgroundColor'))
    set(hObject,'BackgroundColor','white');
end

% --- Executes during object creation, after setting all properties.
function Ricm_CreateFcn(hObject, eventdata, handles)
if ispc && isequal(get(hObject,'BackgroundColor'),
get(0,'defaultUicontrolBackgroundColor'))
    set(hObject,'BackgroundColor','white');
end

% --- Executes on button press in run_lobule.
function run_lobule_Callback(hObject, eventdata, handles)
%read data from the lobule field and sub into equation
s = tf('s');
Cn = str2double(get(handles.Cn, 'String'));
Rn = str2double(get(handles.Rn, 'String'));
Ricm = str2double(get(handles.Ricm, 'String'));
Zlc = (Ricm+s*Ricm*Cn*Rn)/(1+s*Cn*(Rn+Ricm));
Clc = str2double(get(handles.Clc, 'String'));
Rlecm = str2double(get(handles.Rlecm, 'String'));
N =    str2double(get(handles.N, 'String'));
Crbc = str2double(get(handles.Crbc, 'String'));
Rrbc = str2double(get(handles.Rrbc, 'String'));
Rplasma = str2double(get(handles.Rplasma, 'String'));
L =    str2double(get(handles.L, 'String'));
Zblood = (Rplasma+s*Rplasma*Rrbc*Crbc)/(1+s*Crbc*(Rplasma+Rrbc));
Zmv = L*Zblood;
Zlobule = Zmv+N*(Rlecm+s*Rlecm*Clc*Zlc)/(1+s*Clc*(Rlecm+Zlc));
%plot graph
axes(handles.lobule_sim);
bode(Zlobule);
%bode(Zlobule, {2*pi*1, 2*pi*10^8});

% --- Executes during object creation, after setting all properties.
function Clc_CreateFcn(hObject, eventdata, handles)
if ispc && isequal(get(hObject,'BackgroundColor'),
get(0,'defaultUicontrolBackgroundColor'))
```

```
        set(hObject,'BackgroundColor','white');
end

% --- Executes during object creation, after setting all properties.
function Rlecm_CreateFcn(hObject, eventdata, handles)
if ispc && isequal(get(hObject,'BackgroundColor'),
get(0,'defaultUicontrolBackgroundColor'))
        set(hObject,'BackgroundColor','white');
end

% --- Executes during object creation, after setting all properties.
function Crbc_CreateFcn(hObject, eventdata, handles)
if ispc && isequal(get(hObject,'BackgroundColor'),
get(0,'defaultUicontrolBackgroundColor'))
        set(hObject,'BackgroundColor','white');
end

% --- Executes during object creation, after setting all properties.
function Rrbc_CreateFcn(hObject, eventdata, handles)
if ispc && isequal(get(hObject,'BackgroundColor'),
get(0,'defaultUicontrolBackgroundColor'))
        set(hObject,'BackgroundColor','white');
end

% --- Executes during object creation, after setting all properties.
function Rplasma_CreateFcn(hObject, eventdata, handles)
if ispc && isequal(get(hObject,'BackgroundColor'),
get(0,'defaultUicontrolBackgroundColor'))
        set(hObject,'BackgroundColor','white');
end
% --- Executes during object creation, after setting all properties.
function N_CreateFcn(hObject, eventdata, handles)
if ispc && isequal(get(hObject,'BackgroundColor'),
get(0,'defaultUicontrolBackgroundColor'))
        set(hObject,'BackgroundColor','white');
end

% --- Executes during object creation, after setting all properties.
function L_CreateFcn(hObject, eventdata, handles)
if ispc && isequal(get(hObject,'BackgroundColor'),
get(0,'defaultUicontrolBackgroundColor'))
        set(hObject,'BackgroundColor','white');
end
```

```
% --- Executes on button press in tissue_run.
function tissue_run_Callback(hObject, eventdata, handles)
s = tf('s');
Cn = str2double(get(handles.Cn, 'String'));
Rn = str2double(get(handles.Rn, 'String'));
Ricm = str2double(get(handles.Ricm, 'String'));
Zlc = (Ricm+s*Ricm*Cn*Rn)/(1+s*Cn*(Rn+Ricm));
Clc = str2double(get(handles.Clc, 'String'));
Rlecm = str2double(get(handles.Rlecm, 'String'));
N =    str2double(get(handles.N, 'String'));
Crbc = str2double(get(handles.Crbc, 'String'));
Rrbc = str2double(get(handles.Rrbc, 'String'));
Rplasma = str2double(get(handles.Rplasma, 'String'));
L = str2double(get(handles.L, 'String'));
Zblood = (Rplasma+s*Rplasma*Rrbc*Crbc)/(1+s*Crbc*(Rplasma+Rrbc));
Zmv = L*Zblood;
Zlobule = Zmv+N*(Rlecm+s*Rlecm*Clc*Zlc)/(1+s*Clc*(Rlecm+Zlc));
Clobule = str2double(get(handles.Clobule, 'String'));
Rtecm = str2double(get(handles.Rtecm, 'String'));
M = str2double(get(handles.M, 'String'));
K = str2double(get(handles.K, 'String'));
Zvessel = K*Zblood;
Ztissue = Zvessel+M*(Rtecm+s*Rtecm*Clobule*Zlobule)/(1+s*Clobule*(Rtecm+Zlobule));
%plot graph
axes(handles.tissue_sim);
bode(Ztissue);

% --- Executes during object creation, after setting all properties.
function K_CreateFcn(hObject, eventdata, handles)
if ispc && isequal(get(hObject,'BackgroundColor'),
get(0,'defaultUicontrolBackgroundColor'))
      set(hObject,'BackgroundColor','white');
end

% --- Executes during object creation, after setting all properties.
function Clobule_CreateFcn(hObject, eventdata, handles)
if ispc && isequal(get(hObject,'BackgroundColor'),
get(0,'defaultUicontrolBackgroundColor'))
      set(hObject,'BackgroundColor','white');
end

% --- Executes during object creation, after setting all properties.
function Rtecm_CreateFcn(hObject, eventdata, handles)
```

```
if ispc && isequal(get(hObject,'BackgroundColor'),
get(0,'defaultUicontrolBackgroundColor'))
    set(hObject,'BackgroundColor','white');
end

% --- Executes during object creation, after setting all properties.
function M_CreateFcn(hObject, eventdata, handles)
if ispc && isequal(get(hObject,'BackgroundColor'),
get(0,'defaultUicontrolBackgroundColor'))
    set(hObject,'BackgroundColor','white');
end

% --- Executes on button press in electrode_run.
function electrode_run_Callback(hObject, eventdata, handles)
% hObject    handle to electrode_run (see GCBO)
% eventdata  reserved - to be defined in a future version of MATLAB
% handles    structure with handles and user data (see GUIDATA)
s = tf('s');
Rs = str2double(get(handles.Rs, 'String'));
Zcpa = str2double(get(handles.Zcpa, 'String'));
Rct = str2double(get(handles.Rct, 'String'));
Zprobe = Rs + (Zcpa*Rct)/(Zcpa+Rct*s);
%plot graph
axes(handles.electrode_sim);
bode(Zprobe);

% --- Executes during object creation, after setting all properties.
function Rs_CreateFcn(hObject, eventdata, handles)
if ispc && isequal(get(hObject,'BackgroundColor'),
get(0,'defaultUicontrolBackgroundColor'))
    set(hObject,'BackgroundColor','white');
end

% --- Executes during object creation, after setting all properties.
function Rct_CreateFcn(hObject, eventdata, handles)
if ispc && isequal(get(hObject,'BackgroundColor'),
get(0,'defaultUicontrolBackgroundColor'))
    set(hObject,'BackgroundColor','white');
end

% --- Executes during object creation, after setting all properties.
function Zcpa_CreateFcn(hObject, eventdata, handles)
% hObject    handle to Zcpa (see GCBO)
% eventdata  reserved - to be defined in a future version of MATLAB
```

```
% handles      empty - handles not created until after all CreateFcns called

% Hint: edit controls usually have a white background on Windows.
%       See ISPC and COMPUTER.
if ispc && isequal(get(hObject,'BackgroundColor'),
get(0,'defaultUicontrolBackgroundColor'))
    set(hObject,'BackgroundColor','white');
end

% --- Executes on button press in system_run.
function system_run_Callback(hObject, eventdata, handles)
% hObject    handle to system_run (see GCBO)
% eventdata  reserved - to be defined in a future version of MATLAB
% handles    structure with handles and user data (see GUIDATA)
s = tf('s');
Cn = str2double(get(handles.Cn, 'String'));
Rn = str2double(get(handles.Rn, 'String'));
Ricm = str2double(get(handles.Ricm, 'String'));
Zlc = (Ricm+s*Ricm*Cn*Rn)/(1+s*Cn*(Rn+Ricm));
Clc = str2double(get(handles.Clc, 'String'));
Rlecm = str2double(get(handles.Rlecm, 'String'));
N =   str2double(get(handles.N, 'String'));
Crbc = str2double(get(handles.Crbc, 'String'));
Rrbc = str2double(get(handles.Rrbc, 'String'));
Rplasma = str2double(get(handles.Rplasma, 'String'));
L =   str2double(get(handles.L, 'String'));
Zblood = (Rplasma+s*Rplasma*Rrbc*Crbc)/(1+s*Crbc*(Rplasma+Rrbc));
Zmv = L*Zblood;
Zlobule = Zmv+N*(Rlecm+s*Rlecm*Clc*Zlc)/(1+s*Clc*(Rlecm+Zlc));
Clobule = str2double(get(handles.Clobule, 'String'));
Rtecm = str2double(get(handles.Rtecm, 'String'));
M = str2double(get(handles.M, 'String'));
K = str2double(get(handles.K, 'String'));
Zvessel = K*Zblood;
Ztissue = Zvessel+M*(Rtecm+s*Rtecm*Clobule*Zlobule)/(1+s*Clobule*(Rtecm+Zlobule));
Rs = str2double(get(handles.Rs, 'String'));
Zcpa = str2double(get(handles.Zcpa, 'String'));
Rct = str2double(get(handles.Rct, 'String'));
Zprobe = Rs + (Zcpa*Rct)/(Zcpa+Rct*s);
H = Ztissue/(Ztissue+Zprobe);
%plot graph
axes(handles.system_sim);
bode(H);
```

```
% --------------------------------------------------------------------
function file_Callback(hObject, eventdata, handles)
% hObject    handle to file (see GCBO)
% eventdata  reserved - to be defined in a future version of MATLAB
% handles    structure with handles and user data (see GUIDATA)

% --------------------------------------------------------------------
function save_Callback(hObject, eventdata, handles)
% hObject    handle to save (see GCBO)
% eventdata  reserved - to be defined in a future version of MATLAB
% handles    structure with handles and user data (see GUIDATA)
[filename,path] = uiputfile('myfile.m','Save file name');
```